Cancer Letters 293 (2010) 213–219

Contents lists available at ScienceDirect

Cancer Letters

journal homepage: www.elsevier.com/locate/canlet

Captopril and S-nitrosocaptopril as potent radiosensitizers: Comparative study and underlying mechanisms

Bénédicte F. Jordan [a], Julie Peeterbroeck [a], Oussama Karroum [a], Caroline Diepart [a], Julie Magat [a], Vincent Grégoire [b], Bernard Gallez [a,*]

[a] Biomedical Magnetic Resonance Unit, Louvain Drug Research Institute, Université Catholique de Louvain, B-1200 Brussels, Belgium
[b] Laboratory of Molecular Imaging and Experimental Radiotherapy, Avenue Hippocrate 54, Université Catholique de Louvain, B-1200 Brussels, Belgium

ARTICLE INFO

Article history:
Received 21 August 2009
Received in revised form 14 January 2010
Accepted 16 January 2010

Keywords:
Radiotherapy
Tumor
EPR
MRI
S-nitrosocaptopril

ABSTRACT

In an effort to improve the issue of radiotherapy treatments, we tested whether S-nitrosocaptopril, a molecule combining a NO donor and an angiotensin converting enzyme inhibitor (ACE inhibitor), could temporarily improve the hemodynamic status of experimental tumors. We monitored the effect of S-nitrosocaptopril in TLT tumors using non rinvasive magnetic resonance techniques. We identified a time window during which tumor oxygenation was improved, as a result of a combined effect on tumor blood flow and oxygen consumption. Consequently, the administration of S-nitrosocaptopril contributed to the increase in efficacy of radiation therapy, an effect that was not observed with captopril alone.

1. Introduction

Tumor hypoxia is now recognized as a key determinant of treatment outcome for human cancers [1]. It is indeed well established that regions within solid tumors experience mild to severe oxygen deprivation owing to aberrant vascular function and are consequently more refractory to cytotoxic treatments such as radio or chemotherapy [2]. Hypoxia is also involved in the development of a more aggressive phenotype and contributes to metastasis formation [3].

The level of tumor oxygenation depends on the balance between oxygen supply and consumption. Therefore, strategies to reduce tumor hypoxia during radiation treatment (with the goal of increasing radiation sensitivity via the 'oxygen effect') can either involve an increase in blood flow and/or a decrease in oxygen consumption by tumor cells. This approach has been recently considered in pre-clinical models [4–8]. Among them, several vasodilator agents as well as NO (nitric oxide) modulators of tumor hemodynamic parameters have been successfully characterized [9–13]. In those studies, NO-mediated treatments have been investigated for their effects on tumor oxygenation and radiation sensitivity, with the identification of the underlying mechanisms, including: (i) a clear ability of NO to inhibit oxygen consumption by tumor cells; (ii) hemodynamic effects of NO on oxygen supply (tumor blood flow and vessels dilation); and (iii) a likely intrinsic role for NO in vivo as a radiosensitizer.

In the current study, we made the hypothesis that S-nitrosocaptopril, resulting from the S-nitrosylation of captopril and thereby playing a double role of ACE inhibitors (angiotensin converting enzyme inhibitor) and NO donor [14], could be able to temporarily improve tumor hemodynamic status. For that purpose, we monitored the effect of S-nitrosocaptopril, in comparison with captopril, in experimental tumors on: (i) tumor oxygenation, which was assessed by EPR oximetry and 19F-MRI, (ii) tumor blood flow, estimated by the patent blue staining assay; and (iii) tumor cell oxygen consumption, determined by EPR

* Corresponding author. Address: CMFA/REMA, Avenue Mounier 73.40, B-1200 Brussels, Belgium. Tel.: +32 2 7647391; fax: +32 2 7647390.
E-mail address: bernard.gallez@uclouvain.be (B. Gallez).

0304-3835/$ - see front matter © 2010 Elsevier Ireland Ltd. All rights reserved.
doi:10.1016/j.canlet.2010.01.016

oximetry. Finally, in order to evaluate the therapeutic relevance of the drug, a regrowth delay assay was performed after irradiation with 10 Gy of X-rays, and the effects of S-nitrosocaptopril and captopril were compared.

2. Materials and methods

2.1. Treatment and tumor models

Syngeneic TLT (Transplantable mouse Liver Tumor) [15] were injected intramuscularly in the thigh of 5 week-old male NMRI mice (Animalerie facultaire, Université catholique de Louvain, Brussels). For inoculation, approximately 10^6 cells in 0.1 ml of media were injected intramuscularly into the right leg of the mice. Mice developed palpable tumors within a week of inoculation. Tumors were allowed to grow to 8 mm in diameter prior to experimentation. Animals were anesthetized by inhalation of isoflurane mixed with 21% oxygen in a continuous flow (1.5 L/h), delivered by a nose cone. Induction of anesthesia was done using 3% isoflurane. It was then stabilized at 1.8% for a minimum of 15 min before any measurement. The temperature of the animals was kept constant using IR light or by flushing warm air in the MR magnet. Captopril (Sigma–Aldrich) and S-nitrosocaptopril (Alexis Benelux) were administered ip at a dose of 0.046 mmol/kg (corresponding to 10 mg/kg for captopril and 11 mg/kg for S-nitrosocaptopril), diluted in saline or saline with 10% ethanol, respectively. This dose of captopril has been identified earlier by our group as an efficient dose to increase tumor oxygenation [16]. Consequently, the same molar dose was used for S-nitrosocaptopril to allow proper comparison of the effects.

2.2. Tumor oxygenation

2.2.1. EPR oximetry

EPR oximetry relies on the oxygen-dependent broadening of the EPR line width of a paramagnetic oxygen sensor implanted in the tumor [4]. The technique is intended for continuous measurement of local pO_2 without altering the local oxygen concentration. EPR spectra were recorded using an EPR spectrometer (Magnettech, Berlin, Germany) with a low frequency microwave bridge operating at 1.2 GHz and extended loop resonator. Charcoal (Charcoal wood powder, CX0670–1; EM Science, Gibbstown, NJ) was used as the oxygen sensitive probe in all of the experiments [16]. Calibration curves were made by measuring the EPR line width as a function of the pO_2. For this purpose, the charcoal was suspended in a tumor homogenate, and EPR spectra were obtained on a Bruker EMX EPR spectrometer (9 GHz) between 0% and 21% O_2. Nitrogen and air were mixed in an Aalborg gas mixer (Monsey, NY), and the oxygen content was analyzed using a Servomex oxygen analyzer OA540 (Analytic systems, Brussels, Belgium). Mice were injected in the center of the tumor (6 mm diameter) using the suspension of charcoal (100 mg/ml, 50 μL injected, 1–25 μm particle size). EPR measurements were started 2 days after the injection. The tumor under study was placed in the center of the extended loop resonator, the sensitive volume of which extended 1 cm into the tumor mass, using a protocol described previously [4,16]. The localized EPR measurements obtained with the 1.2 GHz (or L band) spectrometer correspond to an average of pO_2 values in a volume of $\sim$10 mm^3.

2.2.2. ^{19}F MRI measurements

MRI was performed with a 4.7*T* (200 MHz, 1H), 40 cm inner diameter bore system (Bruker Biospec, Ettlingen, Germany). A tunable $^1H/^{19}F$ surface coil was used for RF transmission and reception. Parametric images of the spin–lattice relaxation time (T_1) were estimated using a snapshot inversion recovery (SNAP-IR) pulse sequence [17]. The pulse sequence consisted of a non selective hyperbolic secant inversion pulse (10 ms length), followed by acquisition of a series of 512 rapid gradient echo images (repetition time = 10.9 ms, echo time = 4.2 ms, flip angle = 1°, matrix = 32 * 16, field of view = 60 * 30 mm, bandwidth = 12.5 kHz, single thick slice (projection), total acquisition time = 1.5 min) (Jordan, 2009). Raw (*k*-space) data were zero-filled to a matrix size of 64 * 64, resulting in interpolated 64 * 64 images. For each image pixel T_1 was estimated by fitting the standard 3-parameter mono-exponential recovery equation (magnitude data only) describing the signal as a function of inversion time. We denote this computed T_1 as T_1' because the recovery curve is somewhat perturbed by the RF pulses. We then computed $R_1' = \frac{1}{T_1'}$. Calibration of HFB (R_1' with respect to pO_2) was performed by measuring R_1' in three different sealed tubes containing 300 μL HFB respectively bubbled with nitrogen (0% O_2), air (21% O_2), and carbogen (95% O_2) for 20 min in a 37° water bath before measurement. For in vivo studies, HFB was injected into the tumor via an insulin syringe (29G) and deposited along three tracks (3 * 30 μL) encompassing both central and peripheral regions in a coronal plane. HFB was deoxygenated by bubbling nitrogen for 5 min before use. MRI scout images were obtained for both ^1H (200.1 MHz) and ^{19}F (188.3 MHz) to reveal HFB distribution within the tumor. SNAP-IR images were used to measure pO_2 before and after treatment with S-nitrosocaptopril.

2.3. Tumor blood flow

2.3.1. Patent blue staining

Patent blue (Sigma–Aldrich, Belgium) was used to obtain a rough estimate of the tumor perfusion [18] 30 min after treatment with captopril (0.046 mmol/kg), S-nitrosocaptopril (0.046 mmol/kg), or vehicle. This technique involves the injection of 200 μL of Patent blue (1.25%) solution into the tail vein of the mice. After 1 min, a uniform distribution of the staining through the body was obtained and mice were sacrificed. Tumors were carefully excised and cut into size-matched halves. Pictures of each tumor cross section were taken with a digital camera. To compare the stained versus unstained area, an in-house program running on Interactive Data Language (Research Systems Inc., Boulder, CO) was developed. For each tumor, a region of interest (stained area) was defined on the two pictures and the percentage of stained area of the whole cross section was determined. The mean of the percentages

of the two pictures was then calculated and was used as an indicator of tumor perfusion [19].

2.4. Tumor oxygen consumption rate

TLT cells were set in culture in William's medium containing 10% fetal bovine serum, 1% streptomycin/penicillin, and 1.2% glutamine. Cells were collected and cell viability was determined by trypan blue exclusion. An EPR method was used, which has previously been described [10]. Briefly, the spectra were recorded on a Bruker EMX EPR spectrometer operating at 9 GHz. Cells (2×10^7/mL) were suspended in 10% dextran in complete medium in the presence of 1.7 mM of treatment (captopril or S-nitrosocaptopril). A neutral nitroxide, ^{15}N 4-oxo-2,2,6,6-tetramethylpiperidine-d_{16}-^{15}N-1-oxyl at 0.2 mmol/L (CDN Isotopes, Pointe–Claire, Quebec, Canada), was added to 100 μL aliquots of tumor cells that were then drawn into glass capillary tubes. The probe was previously calibrated so that the linewidth measurements could be related to O_2 [10]. The sealed tubes were placed into quartz EPR tubes and the samples were maintained at 37 °C. Because the resulting line width reports on pO_2, it was possible to calculate oxygen consumption rates by measuring the pO_2 in the closed tube as a function of time and subsequently compute the slope of the resulting plot.

2.5. NO spin-trapping in TLT cells

The detection of NO production in a TLT cell suspension was conducted using the NO trapping method with the water soluble iron-MGD complex (iron-*N*-methyl-D-glucamine dithiocarbamate). MGD and iron form a paramagnetic complex with NO ($NO–Fe^{2+}(MGD)_2$), which gives a characteristic anisotropic triplet EPR spectrum [20]. The sodium salt of MGD was from Alexis Biochemicals (Brussels, Belgium). All procedures were carried out under nitrogen to prevent iron(II) from oxidizing. The solvents were degassed with nitrogen before use. Fe(II)-MGD complex was prepared by dissolution in water of MGD sodium salt and iron(II) sulfate. The spin trap solution was added to a TLT cell suspension (2×10^7/ml). S-nitrosocaptopril solution was then added, with final concentrations of 10, 12.5, and 62.5 mM for S-nitrosocaptopril, Fe(II), and ligand, respectively. The EPR spectra were recorded at 310 K on a Bruker EMX EPR spectrometer operating at 9.4 GHz. Typical spectrometer conditions were: incident microwave power, 40 mW; modulation amplitude, 2 Gauss; sweep width, 150 Gauss; and time constant, 5.12 ms.

2.6. Tumor radiation sensitivity

2.6.1. Tumor regrowth delay assay

The tumor bearing leg was irradiated locally with 10 Gy of 250 kV X-rays (RT 250; Philips Medical Systems). Mice were anesthetized, and the tumor was centered in a 3 cm diameter circular irradiation field. When tumors reached 8.0 ± 0.5 mm in diameter, the mice were randomly assigned to a treatment group and irradiated. After treatment, tumors were measured every day until they reached a diameter of 16 mm, at which time the mice were sacrificed. A linear fit to the tumor diameter could be obtained between 8 and 16 mm, which allowed us to determine the time to reach a particular size for each mouse (12 mm).

2.7. Statistical analysis

Results are presented as means ± SEM. Comparisons between groups were analyzed by ANOVA (multiple comparison post tests) since the experiments included more than two groups. P values <0.05 were considered statistically significant.

3. Results

3.1. Effect of captopril and S-nitrosocaptopril on tumor pO_2

The two techniques we used are intended for continuous measurement of the local pO_2 without altering the local oxygen concentration, and allow a real-time study of the oxygen fluctuations in tissues. EPR oximetry is a local measurement but presents the advantage of being the most sensitive and time-resolved, while ^{19}F-MRI oximetry allows oxygen mapping and therefore probes the heterogeneity of response, which is critical for identification of resistant tumor regions.

S-nitrosocaptopril treated mice showed a significant increase in tumor oxygenation from 15 to 60 min post-injection, compared to vehicle treated mice; with a plateau value around 8 mm Hg, as shown by EPR oximetry (Fig. 1). Captopril showed a lower increase in tumor oxygenation, that was still significant from 15 to 60 min post-injection, but that did not go above the radiosensitivity threshold value of 5 mm Hg (Fig. 1) (both controls were stable throughout the experiment, data not shown). The monitoring of tumor pO_2 with ^{19}F-MRI consistently showed a similar time window of enhanced oxygenation after treatment with S-nitrosocaptopril. Fig. 2 shows typical oxygenation maps before, and at 15, 30, and 45 min post-injection of S-nitrosocaptopril with progressive and heterogeneous improvement in tumor pO_2. The histogram analysis shows a large distribution of values before treatment that is still modified after treatment, with a shift of the mean (from 23.5 ± 2.3 to 37.4 ± 2.0 mm Hg) and median (from 18.5 to 31.9 mm Hg) pO_2 on the combined histograms of 15–45 min time points (Fig. 2). ^{19}F-MRI oximetry shows higher absolute pO_2 values than EPR oximetry but both techniques show similar patterns of response after treatment with S-nitrosocaptopril. The size of the sampling volume is likely to be responsible for this discrepancy. This has been reported and discussed earlier in a comparison between ^{19}F-MRI with HFB and fluorescence quenching probes [17]. The time window of improved oxygenation was used to design the "mechanistic experiments" (flow and oxygen consumption measurements) and gives a rationale for

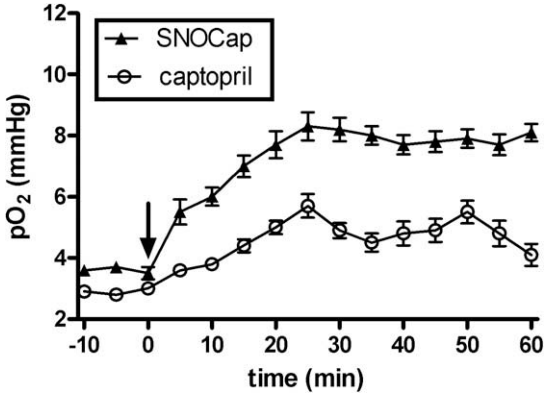

Fig. 1. Evolution of pO_2 in tumors treated with S-nitrosocaptopril or captopril over time, monitored by EPR oximetry.

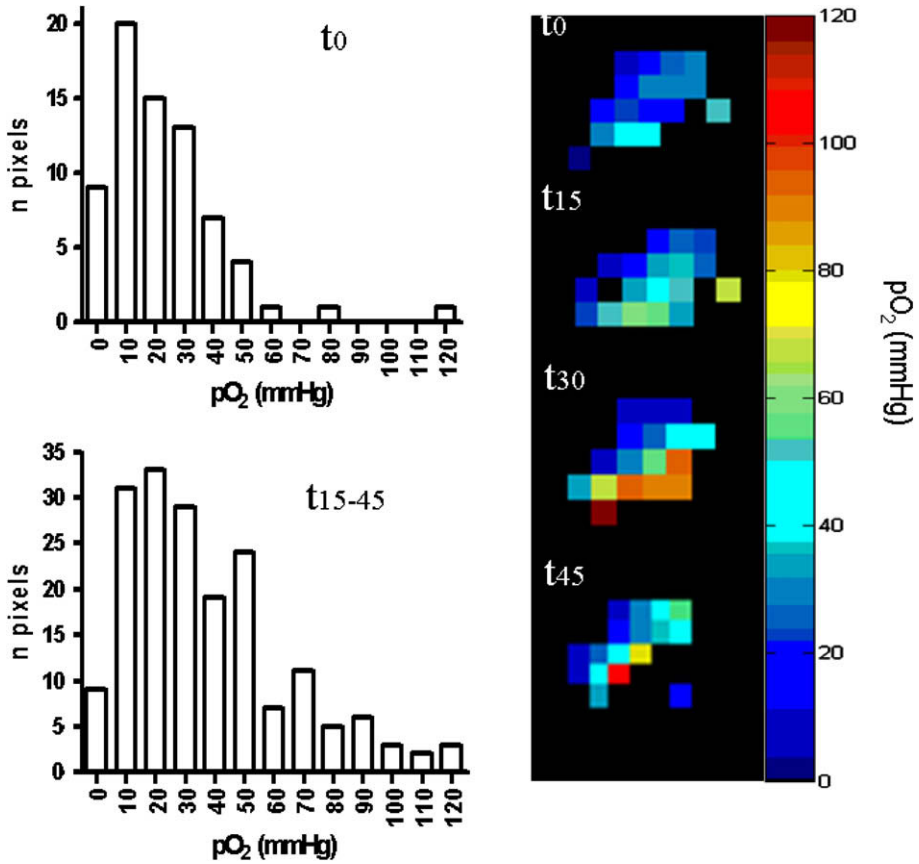

Fig. 2. Typical oxygen maps (^{19}F-MRI) before, and 15–45 min after administration of S-nitrosocaptopril and their corresponding pooled histograms.

the potential use of S-nitrosocaptopril as a co-treatment for radiation therapy. To determine if the increase in tumor oxygenation is the result of an improved blood flow and/or decreased oxygen consumption, patent blue and in vitro EPR experiments were performed.

3.2. Effect of captopril and S-nitrosocaptopril on tumor blood flow

A rough estimate of the tumor perfusion was carried out using the colored area observed in tumors after injection of a dye. This method provides an approximate of relative blood flow but has been validated in the past in comparison with DCE-MRI [7]. Tumors with captopril and S-nitrosocaptopril treatments (30 min time point) stained more positive (87.3 ± 2.2%, n = 10 and 83.2 ± 6.7%, n = 7; respectively) than tumors treated with vehicle (54.1 ± 8.6%, n = 9; Fig. 3). This difference was found to be statistically significant for both groups ($P < 0.01$). This suggests that both drugs are able to acutely improve tumor blood flow, which could be due to the action of the drugs on the tumor co-opted vessels from the host vasculature (“mature” vessels with vascular reactivity).

3.3. Effect of captopril and S-nitrosocaptopril on tumor cell oxygen consumption

TLT cells treated with S-nirosocaptopril consumed oxygen at a significantly slower rate than vehicle treated cells, with a mean slope of −0.904 μM/min and −1.383 μM/min, respectively ($p < 0.05$), whereas the slight decrease in oxygen consumption observed in TLT cells treated with captopril was not significant (Fig. 4). Only S-nirosocaptopril is therefore able to decrease oxygen consumption rate by tumor cells, and not captopril alone, which suggests that the NO moiety of the drug would be responsible for this effect.

3.4. Detection of NO in TLT cell suspension

The spin-trapping experiment in a TLT cell suspension, performed using the NO trapping method with the water soluble iron-MGD complex, was able to show the production of NO in the system, with the characteristic triplet detected as soon as 5 min after preparing the mixture (Fig. 5).

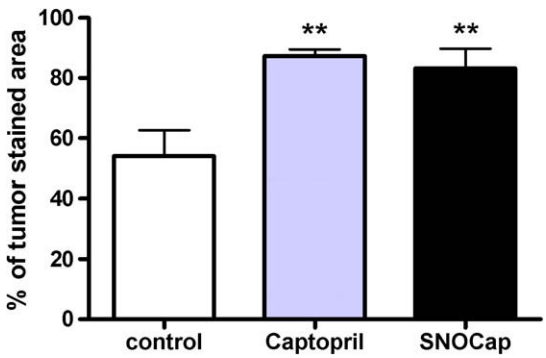

Fig. 3. Effect of S-nitrosocaptopril and captopril on tumor perfusion assessed by patent blue staining 30 min after administration of the treatment. Each bar represents the mean value of tumor percentage of colored area ± SEM for each group.

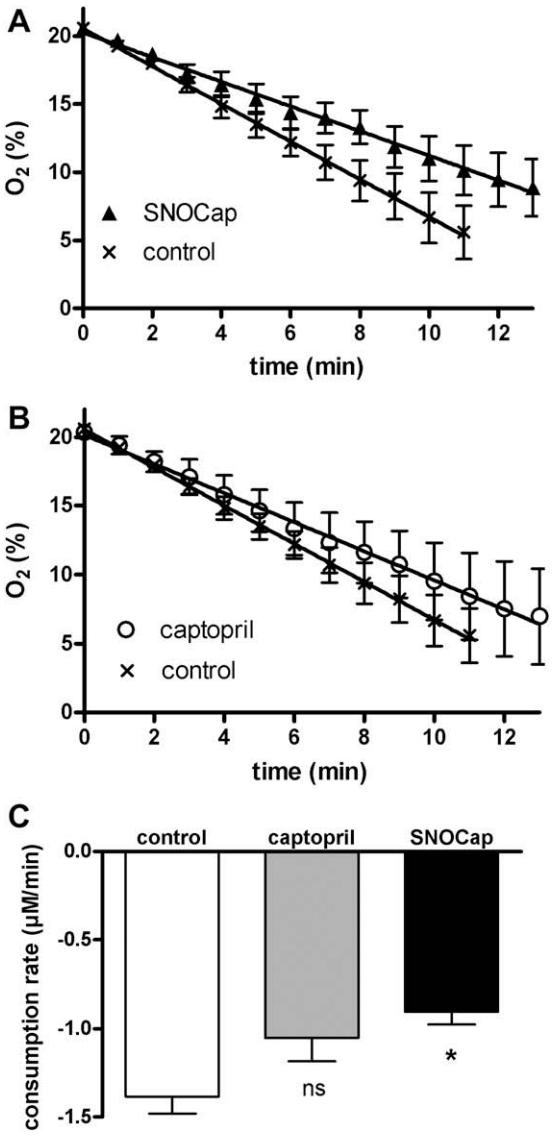

Fig. 4. Effect of S-nitrosocaptopril (A) and captopril (B) on tumor cell oxygen consumption rate. (C) Bar graph representation of the slopes of the linear fit (consumption rates) in (A) and (B).

3.5. Effect of captopril and S-nitrosocaptopril on tumor radiation sensitivity

To assess the therapeutic relevance of the increase in tumor oxygenation after captopril and S-nitrosocaptopril, treated and control tumor bearing mice were irradiated with 10 Gy of X-rays and the tumor regrowth delays were measured. The setup included: (i) three non irradiated groups which were injected either with captopril, S-nitrosocaptopril, or vehicle, at day 0; (ii) two irradiated groups which were submitted to 10 Gy of X-rays 30 min after injection with captopril and S-nitrosocaptopril and; (iii) two tumor clamped irradiated groups with similar treatment protocols (captopril and S-nitrosocaptopril). Tumor clamping is performed by temporary ligation of the leg (during irradiation) and induces complete hypoxia at the time of irradiation. This protocol is used to discriminate between an oxygen effect and a direct radiosensitizing effect of a treatment [21]. The control (non irradiated) groups showed a slight trend of captopril and S-nitrosocaptopril at increasing tumor growth delay, but this was not significant after a single injection at day 0 (Fig. 6A). After irradiation, the time to reach a 12 mm

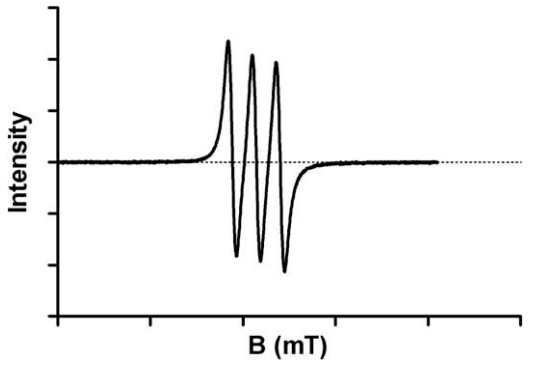

Fig. 5. Typical example of an EPR spectrum corresponding to the paramagnetic complex formed between MGD, iron, and NO (NO–$Fe^{2+}(MGD)_2$), during spin-trapping experiment in TLT cell culture in the presence of S-nitrosocaptopril.

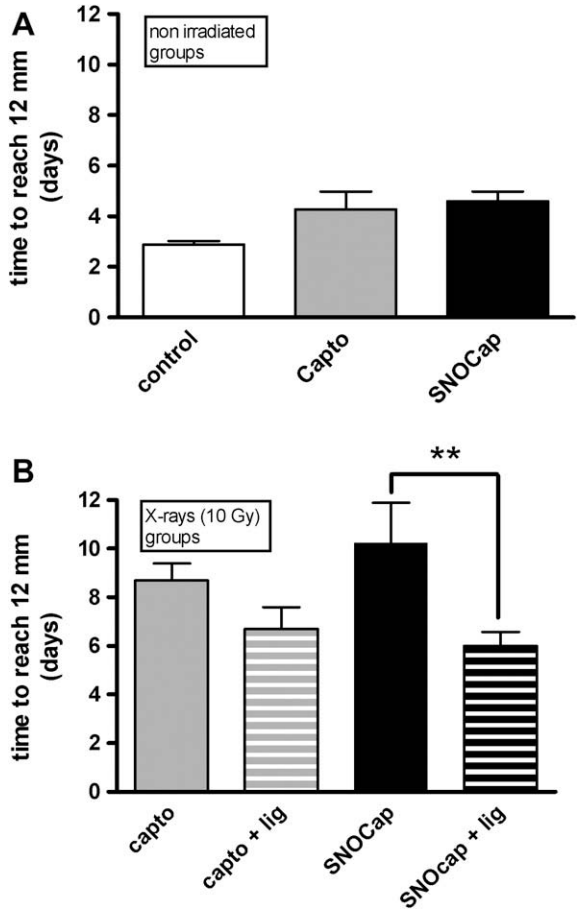

Fig. 6. Regrowth delay assay after irradiation experiment. Bar graph of delays (unit in days) needed to reach 12 mm tumor diameter after treatment with (A) vehicle, S-nitrosocaptopril or captopril; and (B) S-nitrosocaptopril or captopril combined to 10 Gy of X-rays and their corresponding 'hypoxic' (ligated) groups.

tumor diameter was significantly increased in the S-nitrosocaptopril group compared to its "tumor clamped" counterpart (10.2 ± 1.7 days, $n = 7$ vs. 6.0 ± 0.6 days, $n = 6$); whereas the slight difference in regrowth

delays was not significant between the "captopril" and "tumor clamped captopril" groups. This experiment showed that oxygen is necessary for S-nitrosocaptopril to induce a significant regrowth delay after irradiation, and is not due to a direct radiosensitizing effect of the drug.

4. Discussion

Our purpose was to compare captopril and its S-nitrosylated counterpart in order to determine if the combined effect of a NO donor and the vasodilator properties of an ACE inhibitor could have an impact on tumor hemodynamics and could be considered as a relevant co-treatment for radiotherapy. To be efficient, a combination of treatment has to be carefully scheduled, i.e. radiotherapy has to be applied at the exact moment of reoxygenation. This time window can only be identified by the study of key tumor micro-environment parameters, such as oxygenation, oxygen consumption, and perfusion. Therefore, we monitored pO_2 in experimental tumors before and after captopril and S-nitrosocaptopril administration. We reported a significant acute increase (from 20 to 60 min post-injection) in TLT tumor oxygenation using both localized EPR oximetry and oxygen mapping with ^{19}F-MRI. This latter also showed spatial heterogeneity of response within the tumor, with "good responding" and "non responding" regions, that might lead to resistance to therapy. Nevertheless, this 'reoxygenation' window could be exploited to enhance the efficacy of radiation therapy, with a significant increase in regrowth delay after treatment with S-nitrosocaptopril, but not after administration of captopril. This is in accordance with the differential effect of the drugs in terms of tumor pO_2. Mechanistically, the reoxygenation induced by S-nitrosocaptopril resulted from a combined effect on tumor blood flow and oxygen consumption by tumor cells; whereas captopril only significantly influenced tumor blood flow with a lack of effect on oxygen consumption. The effect on oxygen consumption is thus likely due to the 'NO' part of the molecule. Our spin-trapping experiment confirms that NO is released from the system in a tumor cell suspension. It is indeed described that NO regulates mitochondrial respiration by virtue of reversible interactions with cytochrome c oxidase (complex IV in the mitochondrial respiratory chain) [22]. Moreover, we have previously documented the ability of several NO-mediated treatments to modulate tumor oxygen consumption rate in vivo in tumors [10,12]. The improved radiation response after S-nitrosocaptopril is therefore probably the result of the decrease in oxygen consumption rate. Although a direct radiosensitizing effect of NO in vivo has been described after induction of eNOS [10,12,13], we do not think that this direct role would be involved here after administration of exogenous NO since both 'clamped' irradiated groups (captopril and S-nitrosocaptopril) show similar regrowth delays. Also, captopril has been described as a potent inhibitor of experimental tumor growth when administered daily for 3 weeks via an increase in apoptosis [23], and as an inductor of apoptosis in leukemic cell lines [24]. Here, we observed a slight increase in growth delay in the 'non irradiated' groups, but which was not significant after a single injection. It is therefore not likely that the apoptotic properties of captopril would be responsible for the regrowth delay after irradiation combined to a single injection of the drug.

The selective aspect of the approach rely on the fact that tumor tissues are more hypoxic and less perfused than normal tissues, therefore, the relative enhancement in oxygen and blood flow is larger in tumors than in healthy tissues. Moreover, the critical cut off value in terms of pO_2 and radiosensitization is situated between 5 and 10 mm Hg. Therefore, the impact of such an agent able to increase tumor pO_2 above this cut off is substantial compared to normal tissues.

The non physiological NO concentrations that might be reached in tissues following administration of S-nitrosocaptopril could induce hemodynamic side effects. However, the co-treatment planning proposed here is not to compare with side effects of long term NO produced following chemotherapy such as IL-2, which induced hypotensive effects and endothelial damages through the production of NO during the entire course of the treatment [25]. The pro-vascular approach considered here only implies administration of the NO donor drug at the time of irradiation, with an acute and short effect on tumor hemodynamics (less than one hour). It is therefore not likely that systemic chronic side effects would be observed. Nevertheless, it would be critical to find the correct dose that would be able to induce tumor reoxygenation without important acute side effects in a clinical setting. Jia et al. considered the acute and sub acute toxicity in a rodent study and found S-nitrosocaptopril as a safe drug for further clinical trials at therapeutic anti-hypertensive drug dosage [26]. Also, alternative routes of administration could be considered in order to target the tumor and to avoid acute side effects observed with overdosing. Our previous study using insulin as a reversible inductor of eNOS already showed that the combination with irradiation did not induce more toxicity to normal tissues than X-rays alone [27]. This will need to be repeated with S-nitrosocaptopril. Moreover, many pre-clinical steps would be required since the drug has not been characterized in humans yet, although limited experimental and clinical trials on combined therapy with nitrates and captopril have produced promising results for anti-hypertensive therapy [28].

A comparison with a 'simple' NO donor on the same tumor model would give insights on the respective roles of the 'NO' and 'ACEI' contributions of the drug. Isosorbide dinitrate has indeed been described to enhance tumor oxygenation and radiation response in FSaII tumors [11]. Furthermore, spin-trapping experiments would be required to monitor the level of NO in tumors after treatment. In future studies, it would be interesting to evaluate the effect on fractionated radiotherapy with multiple injections of S-nitrosocaptopril, which is closer to the clinical situation. Also, additional tumor models should be considered for further pre-clinical validation. In conclusion, we demonstrated the relevance of the potential use of S-nitrosocaptopril as a co-treatment for radiation therapy in view of

the impact of the drug on experimental tumor oxygenation and radiation sensitivity, and the need for further pre-clinical characterization.

Conflicts of interest

None declared.

Acknowledgments

This work is supported by grants from the Belgian National Fund for Scientific Research (FNRS), the Fonds Joseph Maisin, the Fondation Belge contre le Cancer, the Saint-Luc Foundation, the "Actions de Recherches Concertées-Communauté Française de Belgique-ARC 04/09-317", the «Pôle d'attraction Interuniversitaire PAI VI (P6/38)».

Caroline Diepart is 'Televie' Researcher of the FNRS (Belgian Funds for Scientific Research) and B.F. Jordan is Research Associate of the FNRS.

References

[1] J.A. Bertout, S.A. Patel, M.C. Simon, The impact of O_2 availability on human cancer, Nat. Rev. Cancer 8 (2008) 967–975.
[2] S. Rockwell, I.T. Dobrucki, E.Y. Kim, S.T. Marrison, V.T. Vu, Hypoxia and radiation therapy: past history, ongoing research, and future promise, Curr. Mol. Med. 9 (2009) 442–458.
[3] R.G. Bristow, R.P. Hill, Hypoxia and metabolism. Hypoxia, DNA repair and genetic instability, Nat. Rev. Cancer. 8 (2008) 180–192.
[4] B. Gallez, C. Baudelet, B.F. Jordan, Assessment of tumor oxygenation by electron paramagnetic resonance. principles and applications, NMR Biomed. 17 (2004) 240–262.
[5] N. Crokart, K. Radermacher, B.F. Jordan, C. Baudelet, G.O. Cron, N. Beghein, C. Bouzin, O. Feron, B. Gallez, Tumor radiosensitization by antiinflammatory drugs: evidence for a new mechanism involving the oxygen effect, Cancer Res. 65 (2005) 7911–7916.
[6] N. Crokart, B.F. Jordan, C. Baudelet, G.O. Cron, J. Hotton, K. Radermacher, V. Grégoire, N. Beghein, P. Martinive, C. Bouzin, O. Feron, B. Gallez, Glucocorticoids modulate tumor radiation response through a decrease in tumor oxygen consumption, Clin. Cancer Res. 13 (2007) 630–635.
[7] R. Ansiaux, C. Baudelet, B.F. Jordan, N. Crokart, P. Martinive, J. DeWever, V. Grégoire, O. Feron, B. Gallez, Mechanism of reoxygenation after antiangiogenic therapy using SU5416 and its importance for guiding combined antitumor therapy, Cancer Res. 66 (2006) 9698–9704.
[8] B.F. Jordan, N. Christian, N. Crokart, V. Grégoire, O. Feron, B. Gallez, Thyroid status is a key modulator of tumor oxygenation: implication for radiation therapy, Radiat. Res. 168 (2007) 428–432.
[9] B.F. Jordan, P. Misson, R. Demeure, C. Baudelet, N. Beghein, B. Gallez, Changes in tumor oxygenation/perfusion induced by the no donor, isosorbide dinitrate, in comparison with carbogen: monitoring by EPR and MRI, Int. J. Radiat. Oncol. Biol. Phys. 48 (2000) 565–570.
[10] B.F. Jordan, V. Grégoire, R.J. Demeure, P. Sonveaux, O. Feron, J.A. O'Hara, V.P. Vanhulle, N. Delzenne, B. Gallez, Insulin increases the sensitivity of tumors to irradiation: involvement of an increase in tumor oxygenation mediated by a nitric oxide-dependent decrease of the tumor cells oxygen consumption, Cancer Res. 62 (2002) 3555–3561.
[11] B.F. Jordan, N. Beghein, M. Aubry, V. Grégoire, B. Gallez, Potentiation of radiation-induced regrowth delay by isosorbide dinitrate in FSaII murine tumors, Int. J. Cancer. 103 (2003) 138–141.
[12] B.F. Jordan, P. Sonveaux, O. Feron, V. Grégoire, N. Beghein, C. Dessy, B. Gallez, Nitric oxide as a radiosensitizer: evidence for an intrinsic role in addition to its effect on oxygen delivery and consumption, Int. J. Cancer 109 (2004) 768–773.
[13] P. Sonveaux, B.F. Jordan, B. Gallez, O. Feron, Nitric oxide delivery to cancer: why and how?, Eur J. Cancer. 45 (2009) 1352–1369.
[14] J.P. Cooke, N. Andon, J. Loscalzo, S-nitrosocaptopril II. Effects on vascular reactivity, J. Pharmacol. Exp. Ther. 249 (1989) 730–734.
[15] H.S. Taper, G.W. Woolley, M.N. Teller, M.P. Lardis, A new transplantable mouse liver tumor of spontaneous origin, Cancer Res. 26 (1966) 143–148.
[16] B. Gallez, B.F. Jordan, C. Baudelet, P.D. Misson, Pharmacological modifications of the partial pressure of oxygen in murine tumors: evaluation using in vivo EPR oximetry, Reson. Med. 42 (1999) 627–630.
[17] B.F. Jordan, G.O. Cron, B. Gallez, Rapid monitoring of oxygenation by ^{19}F magnetic resonance imaging: simultaneous comparison with fluorescence quenching, Magn. Reson. Med. 61 (2009) 634–638.
[18] G. Sersa, M. Cemazar, D. Miklavcic, D.J. Chaplin, Tumor blood flow modifying effect of electrochemotherapy with bleomycin, Anticancer Res. 19 (1999) 4017–4022.
[19] R. Ansiaux, C. Baudelet, B.F. Jordan, N. Beghein, P. Sonveaux, J. De Wever, P. Martinive, V. Grégoire, O. Feron, B. Gallez, Thalidomide radiosensitizes tumors through early changes in the tumor microenvironment, Clin. Cancer. Res. 11 (2005) 743–750.
[20] K. Tsuchiya, J.J. Jiang, M. Yoshizumi, T. Tamaki, H. Houchi, K. Minakuchi, K. Fukuzawa, R.P. Mason, Nitric oxide-forming reactions of the water-soluble nitric oxide spin-trapping agent, MGD, Free Radical Biol. Med. 27 (1999) 347–355.
[21] B.F. Jordan, N. Christian, N. Crokart, V. Grégoire, O. Feron, B. Gallez, Thyroid status is a key modulator of tumor oxygenation: implication for radiation therapy, Radiat. Res. 168 (2007) 428–432.
[22] E. Clementi, G.C. Brown, N. Foxwell, S. Moncada, On the mechanism by which vascular endothelial cells regulate their oxygen consumption, Proc. Natl. Acad. Sci. USA 96 (1999) 1559–1562.
[23] S. Attoub, A.M. Gaben, S. Al-Salam, M.A. Al Sultan, A. John, M.G. Nicholls, J. Mester, G. Petroianu, Captopril as a potential inhibitor of lung tumor growth and metastasis, Ann. NY. Acad. Sci. 1138 (2008) 65–72.
[24] S. De, C.E. la Iglesia Iñigo, M.T. López-Jorge, A. Gómez-Casares, P. Lemes Castellano, J. Martín Cabrera, A. López Brito, T. Suárez Cabrera, Molero. Labarta, Induction of apoptosis in leukemic cell lines treated with captopril, trandolapril and losartan: a new role in the treatment of leukaemia for these agents, Leuk. Res. 33 (2009) 810–816.
[25] G.M. Buga, L.J. Ignarro, Nitric oxide and cancer, in: Louis J. Ignarro (Ed.), Nitric Oxide Biology and Pathobiology, Academic Press, London, 2000, pp. 895–920.
[26] L. Jia, R. Pei, M. Lin, X. Yang, Acute and subacute toxicity and efficacy of S-nitrosylated captopril, an ACE inhibitor possessing nitric oxide activities, Food Chem. Toxicol. 39 (2001) 1135–1143.
[27] B.F. Jordan, N. Beghein, N. Crokart, C. Baudelet, V. Grégoire, B. Gallez, Preclinical safety and antitumor efficacy of insulin combined with irradiation, Radiother. Oncol. 81 (2006) 112–117.
[28] J.S. Juggi, E. Koenig-Berard, P. Vitou, Vasodilator therapy: interaction of nitrates with angiotensin-converting enzyme inhibitors, Can. J. Cardiol. 7 (1991) 419–425.